

Confined optical modes in photonic wires

A. Kuther, M. Bayer, T. Gutbrod, and A. Forchel

Technische Physik, Universität Würzburg, Am Hubland, D-97074 Würzburg, Germany

P. A. Knipp

Christopher Newport University, Newport News, Virginia 23606

T. L. Reinecke

Naval Research Laboratory, Washington DC 20375

R. Werner

Technische Physik, Universität Würzburg, Am Hubland, D-97074 Würzburg, Germany

(Received 26 May 1998; revised manuscript received 30 July 1998)

The confined optical modes in photonic wires formed by lithography of planar microcavities are studied by angle-resolved photoluminescence spectroscopy. These modes exhibit dispersion along the length of the wire and are confined for motion perpendicular to the wires in plane. Polarization-dependent spectroscopy shows a splitting between modes with electric field along and perpendicular to the wires, which is in agreement with detailed calculations. [S0163-1829(98)06148-7]

I. INTRODUCTION

In recent years there has been considerable work on the photonic properties of planar semiconductor microcavities.¹⁻¹⁷ Typically highly reflecting Bragg mirrors confine the light vertically in such a way that there is a single mode of interest for a broad frequency range for motion in this direction. The motion in the plane, by contrast, is extended and has dispersion given by $E = \hbar c k_{\parallel}$, where k_{\parallel} is the wave vector along the plane. The interest in these systems arises in part from the opportunity to control the electromagnetic spectrum by restricting the modes in the vertical direction. In this way, for example, the spontaneous and stimulated emission into the photon spectrum is modified. It is interesting to note the analogy between the discretization of the vertical modes of such cavities and the electronic confined states of quasi-two-dimensional quantum wells, which have been a main area of semiconductor research in the past two decades.¹⁸

In addition, there has been much interest in systems in which the photon spectrum is fully discretized, such as microwave studies of atoms in optical cavities.¹⁸ In this case the optical spectrum can be limited to a single fully confined mode, and optical recombination rates and spontaneous emission can be strongly modified. During the past few years it has been demonstrated that fully confined optical modes in the near infrared can be observed in micron-sized lithographically patterned planar cavities in semiconductors.^{19,20} In these cases the optical modes are sharp resonances corresponding to full three-dimensional confinement with the lateral confinement arising from the large refractive index differences between the cavity and vacuum. The photonic modes of these structured microcavities can be thought of as analogous to the discrete states of electronic quantum dots of current interest, and they are often called photonic dots for this reason.

Very recently, photonic wire structures have been fabricated and the formation of cavity polaritons has been studied

by angle-dependent photoluminescence spectroscopy.²¹ These structures have modes which are extended in the direction along the wires and show dispersion in this direction and which are discretized in the direction perpendicular to the wires. In this sense they are an intermediate case between the planar cavity and the fully quantized dots.

Here we study the confined optical modes in photonic wire structures by angle-dependent spectroscopy from which we obtain insight into the field distributions inside the cavity. An interesting feature shows up in polarization-dependent luminescence where we see a splitting between modes which have different polarizations of the electric field. We trace this splitting to the effects of the boundaries in the two directions for the electric fields polarized along and perpendicular to the wires. This feature is a consequence of the vector nature of the modes of Maxwell's equations.

II. RESULTS AND DISCUSSION

A. Samples

A planar λ cavity consisting of a GaAs layer of thickness 250 nm sandwiched between two high reflectance mirrors made of alternating GaAs and AlAs layers was used for the fabrication of photonic wires. In the center of the GaAs layer, a 7 nm wide $\text{In}_{0.14}\text{Ga}_{0.86}\text{As}$ quantum well was placed which serves as an optically active medium. In order to obtain quasi-one-dimensional confinement, photonic wires were fabricated by lithography and etching.²² Different from the wires in Ref. 21, the cavity was etched not only through the top reflector but also through the GaAs layer down to the top of the bottom reflector. The lower mirror remained essentially unetched. In comparison, this deeper etching results in a slightly enhanced confinement of the optical modes. The lateral sizes of the wires ranged from about 5.25 μm down to 0.95 μm . Figure 1 shows a scanning electron micrograph of an array of photonic wires with a width of 0.95 μm .²³ On

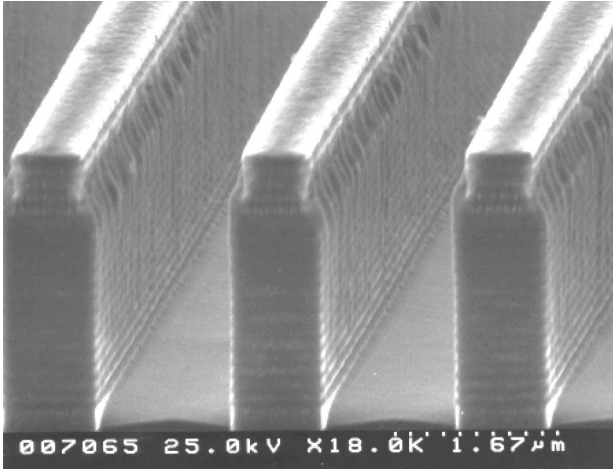


FIG. 1. Scanning electron micrograph of a photonic wire fabricated from lateral patterning of a planar microcavity. The width of the wire is about $0.95 \mu\text{m}$.

top of the structures the alternating GaAs and AlAs mirror layers are seen, followed by the GaAs cavity. The top mirror consists of 19 GaAs/AlAs layers and the bottom mirror of 21 layers.

The samples were mounted into the helium insert of an optical cryostat at $T=5 \text{ K}$. An Ar^+ laser was used for optical excitation of the photonic wires. When angle resolution was not being studied, the luminescence was collected within an angle of about 15° relative to the normal of the cavity. The emission then was dispersed by a double monochromator with a focal length of 1 m and detected by a Peltier-cooled GaAs photomultiplier interfaced with a photon counting system.

B. Angle-resolved studies

In an unpatterned cavity, the energies of the photon modes with free dispersion in the cavity plane are given by

$$E(k_x, k_y) = \sqrt{E_0^2 + \frac{\hbar^2 c_0^2}{\varepsilon} k_{\parallel}^2}, \quad (1)$$

where E_0 is the energy of the fundamental cavity mode determined by the height of the GaAs λ cavity. $k_{\parallel} = \sqrt{k_x^2 + k_y^2}$ is the photon wave number in the cavity plane and ε is the dielectric constant.

In the photonic wires the electric fields are confined in the direction of the wire width as a result of the large refractive index change at the wire boundary. We have made detailed numerical calculations using the boundary element method^{20,24} of the electric fields of these systems as a function of wire size. We find that the electric field distributions inside the structures are given by $\mathcal{E}(x, y) \propto \exp(ik_x x) \times \mathcal{E}(y)$ with the photon wave number k_x along the wire. The confined electric field distributions can be approximated by $\mathcal{E}(y) \propto \cos k_y y$ or $\mathcal{E}(y) \propto \sin k_y y$, where $k_y = (\pi/L_y)(n_y + 1)$, $n_y = 0, 1, \dots$. The frequencies of the confined modes are therefore

$$E_{n_y}(k_x) = \sqrt{E_0^2 + \frac{\hbar^2 c_0^2}{\varepsilon} \left(\frac{\pi^2}{L_y^2} (n_y + 1)^2 + k_x^2 \right)}. \quad (2)$$

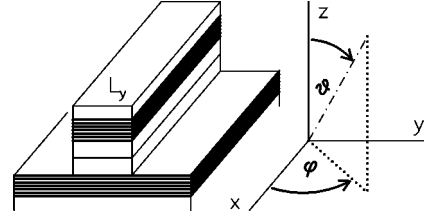


FIG. 2. Definition of the angles ϑ and φ giving the direction of detection relative to the photonic wire shown schematically in the left part of the figure.

Physically Eq. (2) indicates that discrete wave vectors are confined laterally, in agreement with the results reported in Ref. 21.

Angle-resolved photoluminescence studies can be used to investigate the electromagnetic field distribution in the photonic wires in a similar way as was recently done to study the in-plane dispersion of the polariton branches in a planar cavity⁶ and in photonic wires.²¹ In these experiments the emission within a narrow solid angle is detected using an aperture which can be moved parallel to the cavity plane. The distance of the aperture from the sample was about 20 cm in the experiments. With a diameter of the aperture of 4 mm, an angle resolution of about 1° is obtained. The direction of detection is defined by two angles, the polar angle ϑ and the azimuth angle φ , shown schematically in Fig. 2. Each set of angles (ϑ, φ) corresponds to a photon wave vector $k_x = k \sin \vartheta \cos \varphi$ along the wire with $k = E/(\hbar c_0) \sqrt{\varepsilon}$. The detection angle ϑ outside the wire and the polar angle ϑ_i inside are connected by the law of diffraction, $\sin \vartheta = \sqrt{\varepsilon} \sin \vartheta_i$.²⁵

Figure 3(a) shows photoluminescence spectra of $5.25 \mu\text{m}$ wide wires for $\varphi = 90^\circ$, that is with detection normal to the wires.^{26,27} For this direction of detection the energies of the photon modes do not vary with increasing ϑ , giving clear evidence for the confinement normal to the wire axis. However, the emission intensities from each mode in Fig. 3(a) depend on the detection angle, and higher confined photon modes appear at larger angles. For example, the ground-state emission is maximum for $\vartheta = 0$ and then drops continuously to zero with increasing ϑ . The emission intensity for the first excited mode is maximum at about $\vartheta = 8^\circ$ and that of the second excited mode has its maximum at $\vartheta = 14^\circ$.

Figure 3(b) shows angle-resolved spectra of photonic wires with a width of $5.25 \mu\text{m}$ for $\varphi = 0$, where the angle ϑ was varied in the plane given by the wire axis and the cavity normal. For this wire orientation, emission mainly from the ground photon mode $n_y = 0$ is observed. The $\vartheta = 0$ spectrum consists of the emission from the photon mode $n_y = 0$ and $k_x = 0$. With increasing ϑ the emission shifts to higher energies according to the dispersion relation in Eq. (2).²⁸

The far-field emission from an optical mode is given by the Fourier transform of the electric field distribution $\mathcal{E}(x, y)$ inside the wire.^{29,30} The emission intensity at the detector is thus given by

$$I(\vartheta, \varphi) = \left| \int \mathcal{E}(x, y) \exp(i(\kappa_x x + \kappa_y y)) dx dy \right|^2, \quad (3)$$

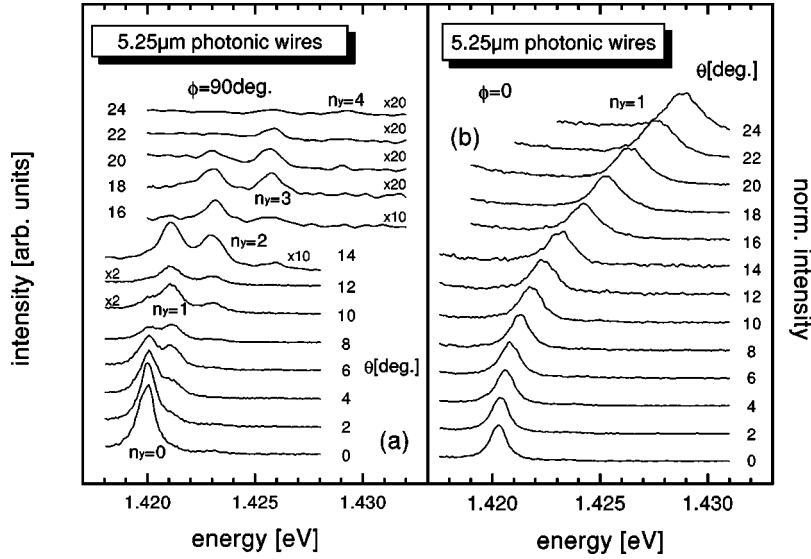


FIG. 3. (a) Angle-resolved spectra of 5.25 μm wide photonic wires. The polar angle ϑ was varied with the azimuth angle fixed at $\varphi = 90^\circ$. (b) Same as in (a) but for a dot orientation of $\varphi = 0^\circ$.

where κ_x, κ_y are related to the observation directions by $\kappa_x = k \sin \vartheta \cos \varphi$ and $\kappa_y = k \sin \vartheta \sin \varphi$. From the general form of the electric field $\mathcal{E}(x, y)$ in photonic wires we obtain

$$I(\vartheta, \varphi) \propto \delta(\kappa_x - k_x) \times \left| \int \mathcal{E}(y) \exp(i\kappa_y y) dy \right|^2. \quad (4)$$

We see that the emission from the mode with wave vector k_x can be observed only in the direction $\sin \vartheta \cos \varphi = k_x/k$. With the simple forms of the confined electric field distributions discussed above, we can calculate the intensities from the integral in Eq. (4) analytically.

The calculated polar angle dependences of the emission intensities of the four lowest optical modes of a 5.25 μm wide photonic wire are compared to the experimental data in Fig. 4.³¹ The observation orientation is perpendicular to the length of the wire ($\varphi = 90^\circ$), for which $\kappa_y = k \sin \vartheta$. The field distribution of each confined mode causes characteristic dependences of the emission on the detection direction. In contrast to spatially extended modes, the Fourier transform of a localized field distribution has an extended distribution in k space. Therefore emission from each confined optical mode is observed over an extended range of angles ϑ . The

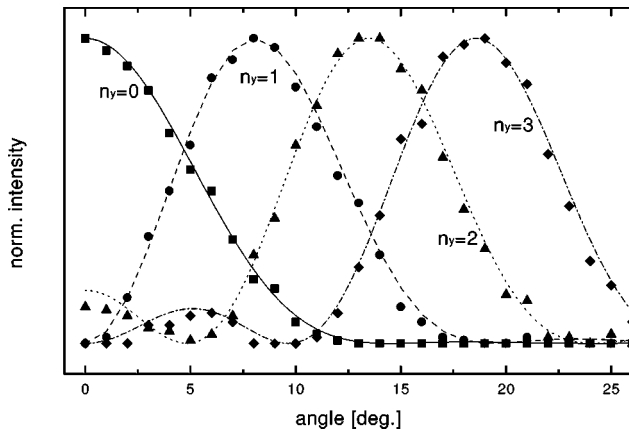


FIG. 4. Variation of the emission intensities of the four lowest confined photon modes in a 5.25 μm wide wire with the polar angle ϑ for $\varphi = 90^\circ$. Symbols give the experimental data, lines give the results of calculations.

ground mode field distribution consists mainly of Fourier components around $k=0$. The excited photon modes contain Fourier components with larger wave numbers, because their field distributions vary more strongly in the confinement region. Therefore the emission shifts to larger angles for the excited modes, as observed in Fig. 3. The emission from each mode becomes maximum when the direction of detection is given by the confined wave number, $k \sin \vartheta = \pi/L_y(n_y + 1)$, which is in good agreement with the calculations.

C. Fine-structure splitting

The vector nature of the electromagnetic fields provides an interesting additional degree of freedom beyond that, for example, of the scalar Schrödinger equation. In order to investigate this aspect of the behavior of the present systems, we have done polarization-dependent studies of the photoluminescence of the wires. The results are shown in Fig. 5, where the solid line corresponds to polarization of the electric field along the length of the wires and the dotted line to

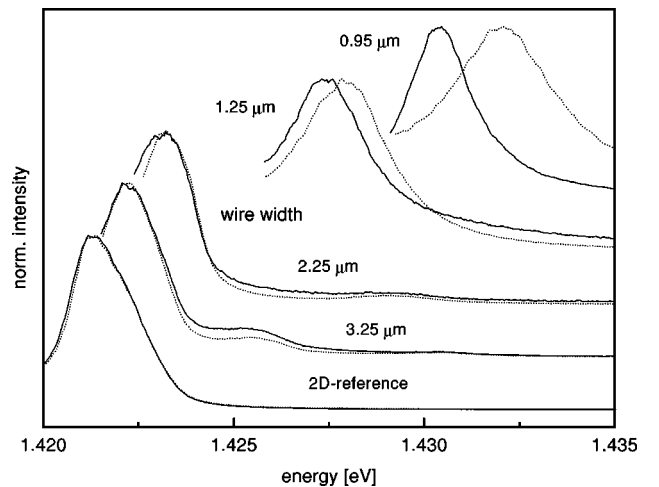


FIG. 5. Linearly polarized photoluminescence spectra of photonic wires of varying widths. The solid lines give the traces for polarization parallel, the dotted lines those for polarization normal to the wires.

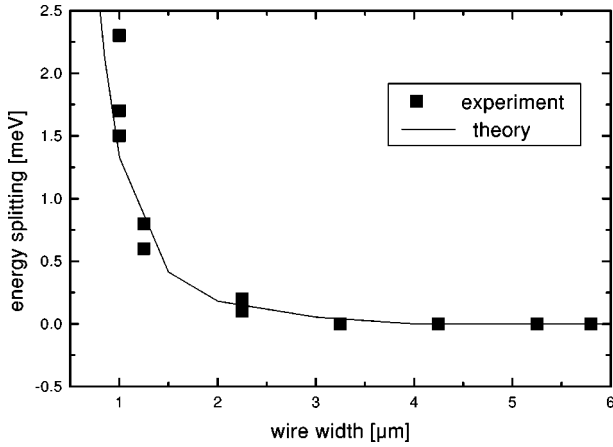


FIG. 6. Energy splitting between the ground optical modes with polarizations perpendicular and parallel to the photonic wires.

polarization perpendicular to the length of the wires. Results are given there for an unpatterned sample and for several wire widths from $3.25 \mu\text{m}$ to $0.95 \mu\text{m}$. A splitting between the two polarizations is observed as the width of the wire is reduced. The experimental results for the width dependence of the splitting are shown in Fig. 6.

In order to understand this observed splitting, it is necessary to go beyond the simple description given above for the fields by including fully the boundary conditions and penetration of the fields outside of the cavities. In these systems the energy of the mode in the unpatterned cavity given by E_0 in Eq. (2) is much larger than the lateral confinement energy in the etched systems, and this allows us to separate the motion in the z direction from that in the plane of the cavity (Fig. 2). In the present wires the motion along the wire (x direction) can be separated exactly from that perpendicular to it (y direction). Then the one-dimensional problem in the y direction including the penetration of the fields outside of the wires can be solved analytically.

The fields in these wires bear a resemblance to those of a dielectric waveguide,³² and the modes here can be separated into TE and TM modes having, respectively, zero electric and zero magnetic fields in the z direction. The TE modes have an electric field in the x direction and a magnetic field predominantly in the y direction and vice versa for the TM modes. The frequencies of these modes are determined by applying the usual boundary conditions at the vacuum/semiconductor interface on the oscillating electric and magnetic fields: The normal component of the dielectric displacement has to be continuous across the interface, while for the electric field the tangential component must be continuous. Continuity must also be fulfilled for the normal component of the magnetic induction and the tangential component of the magnetic field. The energies of the modes are given by $\hbar cK$, where for TE modes K is given by

$$\cot\left(\frac{L_y}{2}\sqrt{\varepsilon K^2 - k^2}\right) - \frac{\sqrt{\varepsilon K^2 - k^2}}{\sqrt{k^2 - K^2}} = 0 \quad (5)$$

and for TM modes it is given by

$$\cot\left(\frac{L_y}{2}\sqrt{\varepsilon K^2 - k^2}\right) - \frac{\sqrt{\varepsilon K^2 - k^2}}{\varepsilon\sqrt{k^2 - K^2}} = 0. \quad (6)$$

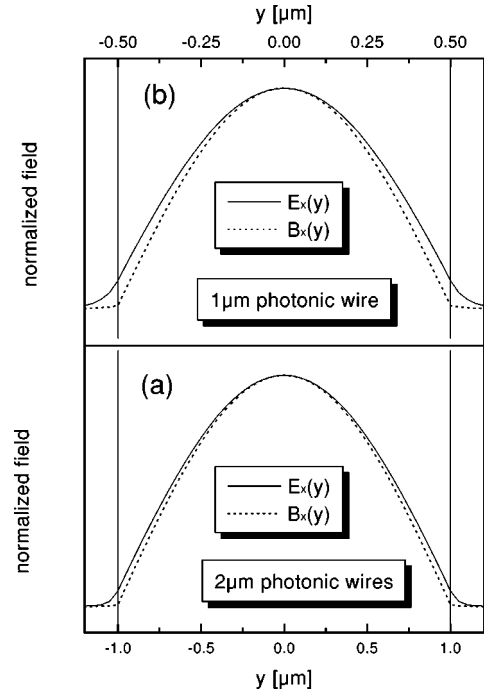


FIG. 7. Field distribution of the TE mode $E_x(y)$ and the TM mode $B_x(y)$ along the y direction in $2 \mu\text{m}$ (a) and $1 \mu\text{m}$ (b) wide photonic wires.

Here $k = (\sqrt{\varepsilon}/\hbar c)E_0$. A factor of ε appears in the denominator of Eq. (6) and not in Eq. (5) due to the boundary condition on the dielectric displacement in the y direction in that case.

The calculated results for the y dependences of the electric and magnetic fields in the x direction for the lowest TE and TM modes [$E_x(y)$ and $B_x(y)$, respectively] of wires with $1 \mu\text{m}$ and $2 \mu\text{m}$ width are shown in Fig. 7. In both cases B_x penetrates less into the vacuum region as a result of the boundary condition on the electric field which is predominantly perpendicular to the interface for this mode. As a result of the increased confinement, the TM mode is higher in energy. For $2 \mu\text{m}$ wide wires the difference of the field distribution between the TE and the TM mode is rather small due to the small field amplitude at the interface and therefore also the energy difference between these modes is small. For $1 \mu\text{m}$ wide wires the confinement of the TM mode still is strong whereas the TE mode penetrates significantly into vacuum resulting in an enhanced energy splitting of the modes. This is consistent with the experimental observation that the mode with electric field polarized perpendicular to the length of the wire is higher in energy. The calculated wire width dependence of the splitting between these two modes is shown in Fig. 6 along with the experimental data. It is seen that these results account well for the observed wire width dependence of the data. The calculated results are also in agreement with those of calculations using the boundary element method described in Ref. 24.

III. SUMMARY

In summary, we have fabricated photonic wires, in which the electromagnetic fields are confined along two spatial directions. The photon modes in the wires can be studied by

angle-resolved photoluminescence spectroscopy which gives direct evidence for the confinement of the photon modes. For small wire widths a splitting of the modes with polarizations parallel and perpendicular to the wires was observed, which arises from the influence of the boundary conditions on these fields at the semiconductor vacuum interface. Thus we have obtained quantitative insight into the optical modes of pho-

tonic wires, which may be considered as intermediate systems between planar cavities and photonic dots.

ACKNOWLEDGMENTS

This work was supported by the State of Bavaria and by the U.S. Office of Naval Research.

- ¹H. Yokoyama, K. Nishi, T. Anan, H. Yamada, S. D. Brorson, and E. P. Ippen, *Appl. Phys. Lett.* **57**, 2814 (1990).
- ²G. Björk, S. Machida, Y. Yamamoto, and K. Igeta, *Phys. Rev. A* **44**, 669 (1991).
- ³C. Weisbuch, M. Nishioka, A. Ishikawa, and Y. Arakawa, *Phys. Rev. Lett.* **69**, 3314 (1992).
- ⁴R. P. Stanley, R. Houdré, U. Oesterle, M. Ilegems, and C. Weisbuch, *Phys. Rev. A* **48**, 2246 (1993).
- ⁵V. Savona, Z. Hradil, A. Quattropani, and P. Schwendimann, *Phys. Rev. B* **49**, 8774 (1994).
- ⁶R. Houdré, C. Weisbuch, R. P. Stanley, U. Oesterle, P. Pellandini, and M. Ilegems, *Phys. Rev. Lett.* **73**, 2043 (1994).
- ⁷I. Abram and J. L. Oudar, *Phys. Rev. A* **51**, 4116 (1995).
- ⁸H. Wang, J. Shah, T. C. Damen, W. Y. Jan, J. E. Cunningham, M. Hong, and J. P. Mannaerts, *Phys. Rev. B* **51**, 14 713 (1995).
- ⁹R. Houdré, J. L. Gibernon, P. Pellandini, R. P. Stanley, U. Oesterle, C. Weisbuch, J. O’Gorman, B. Roycroft, and M. Ilegems, *Phys. Rev. B* **52**, 7810 (1995).
- ¹⁰F. Tassone, C. Piermarocchi, V. Savona, A. Quattropani, and P. Schwendimann, *Phys. Rev. B* **53**, 7642 (1996).
- ¹¹R. P. Stanley, R. Houdré, C. Weisbuch, U. Oesterle, and M. Ilegems, *Phys. Rev. B* **53**, 10 995 (1996).
- ¹²V. Savona, F. Tassone, C. Piermarocchi, A. Quattropani, and P. Schwendimann, *Phys. Rev. B* **53**, 13 051 (1996).
- ¹³P. Kinsler and D. M. Whittaker, *Phys. Rev. B* **54**, 4988 (1996).
- ¹⁴D. M. Whittaker, P. Kinsler, T. A. Fisher, M. S. Skolnick, A. Armitage, A. M. Afshar, M. D. Sturge, J. S. Roberts, G. Hill, and M. A. Pater, *Phys. Rev. Lett.* **77**, 4792 (1996).
- ¹⁵F. Jahnke, M. Kira, S. W. Koch, G. Khitrova, E. K. Lindmark, T. R. Nelson, Jr., D. V. Wick, J. D. Berger, O. Lyngnes, H. M. Gibbs, and K. Tai, *Phys. Rev. Lett.* **77**, 5257 (1996).
- ¹⁶A. Armitage, T. A. Fisher, M. S. Skolnick, D. M. Whittaker, P. Kinsler, and J. S. Roberts, *Phys. Rev. B* **55**, 16 395 (1997).
- ¹⁷D. Baxter, M. S. Skolnick, A. Armitage, V. N. Astratov, D. M. Whittaker, T. A. Fisher, J. S. Roberts, D. J. Mowbray, and M. A. Kaliteevski, *Phys. Rev. B* **56**, 10 032 (1997).
- ¹⁸See, for example, *Confined Electrons and Photons, New Physics and Applications*, edited by E. Burstein and C. Weisbuch, NATO Advanced Study Institute Series B: Physics (Plenum, New York, 1995).
- ¹⁹J. M. Gérard, D. Barrier, J. Y. Marzin, R. Kuszelewicz, L. Manin, E. Costard, V. Thierry-Mieg, and T. Rivera, *Appl. Phys. Lett.* **69**, 449 (1996).
- ²⁰J. P. Reithmaier, M. Röhner, H. Zull, F. Schäfer, A. Forchel, P. A. Knipp, and T. L. Reinecke, *Phys. Rev. Lett.* **78**, 378 (1997).
- ²¹A. I. Tartakovskii, V. D. Kulakovskii, A. Forchel, and J. P. Reithmaier, *Phys. Rev. B* **57**, 6807 (1998).
- ²²Details of the fabrication process are given in M. Röhner, J. P. Reithmaier, A. Forchel, F. Schäfer, and H. Zull, *Appl. Phys. Lett.* **71**, 488 (1997).
- ²³The width of the topmost part of the upper mirror is slightly smaller than the wire width due to damage from etching. However, this narrowing does not affect the optical modes significantly because from transfer matrix calculations we find that the electric field amplitude in this part of the mirror is small.
- ²⁴P. A. Knipp and T. L. Reinecke, in *Proceedings of the 23rd International Conference on the Physics of Semiconductors, Berlin, 1996*, edited by M. Scheffler and R. Zimmermann (World Scientific, Singapore, 1996) p. 3131; *Phys. Rev. B* **54**, 1880 (1996).
- ²⁵In general, radiation from the photonic wires can be emitted through the top reflector or through the wire sidewalls. For the rather small detection angles in the angle-resolved studies, almost all emission comes from the top mirror for large wire widths as $5.25\ \mu\text{m}$ studied here. For small wire widths below $1\ \mu\text{m}$ also the radiation from the sidewalls becomes important in the studied range of angles. Then the simple analysis of the experiments connecting the detection angle with the photon wave number by the law of diffraction is not valid.
- ²⁶The absolute emission intensities from the several photon modes differ because they depend on the coupling to the electronic excitations and this coupling varies with the energy of the modes. Further, low-energy modes are more populated due to relaxation into them. To see higher-lying modes in Fig. 3 the corresponding spectra have been scaled by a factor indicated at each spectrum.
- ²⁷The polarization of the emission spectra in Fig. 3 is parallel to the photonic wires. However, for the wire width of $5.25\ \mu\text{m}$ here the field distributions for polarization normal and parallel to the wires are identical (see also Sec. II C). Thus the angle dependences are the same for both field orientations. For smaller wires the TM mode is more strongly confined than the TE mode resulting in a distribution of the emission over a wider range of angles.
- ²⁸The half-width of the photon emission lines increases with increasing ϑ . We attribute this increase to the decrease of the reflectivity of the upper mirror with increasing incidence angle ϑ .
- ²⁹See, for example, E. Hecht and A. Zajac, *Optics* (Addison-Wesley, Reading, 1974).
- ³⁰The emission from different structures in the photonic wire array is incoherent in the present photoluminescence studies. Coherency of the emission from the wire array would result in an emission pattern corresponding to a diffraction grating.
- ³¹The maxima of the emission intensities of the different photon modes have been normalized to unity because the intensities from each optical mode cannot be easily compared (Ref. 25).
- ³²J. D. Jackson, *Classical Electrodynamics* (John Wiley & Sons, New York, 1967), Chap. 8.